

Aeroelasticity Consideration in Aerodynamic Adaptation of Wing

C.Mohanraj^{1*}, J.Osanna¹

¹ Department of Aerospace Engineering Periyar Maniammai University, Tanjore, India.

ABSTRACT: *The need for measuring aerodynamic efficiency in aircraft design has a challenge for designers for decades. This study makes an attempt to achieve this objective by a novel concept of adding multiple trailing edge flaps. The project makes a modest try to make a modification in existing conventional design concepts. Currently, I used seven trailing edge flaps per wing. The need for multiple trailing edge flaps is to maintain elliptical lift distribution throughout the cruise of the aircraft flight. Measuring aerodynamic efficiency was a complex problem because of fluid- structure interaction involved in the analysis. The study incorporates the fluid structure interaction and its aeroelastic effects on the design. The aeroelastic analysis neglects inertia force and thus static aeroelastic analysis is involved for simplifying the analysis. The theoretical analysis began with relevant equations from Thin Aerofoil theory and Slender Beam theory. The equations from these theories are combined to get the closed form of solution that accounts for wing twist in the calculation of flap angles to create a desired c_l distribution along the wing. Next the FEA model is presented and the method to find the structural properties using FEA is presented. The structural properties are also calculated using standard Aircraft Structures method and the results were compared.*

Keywords: *Aeroelasticity, Flaps, Fluid structure interaction.*

I. INTRODUCTION

Adaptive wings are generating considerable interest due to their potential for drag reduction in 1-g flight and wing load alleviation during maneuvering flight. Recent research has shown that series of flaps placed along the trailing edge of the wing can be used to optimize the wing across several flight conditions. Without these multiple trailing edge flaps, wing can be optimized for flight at one particular condition and suffer deficiencies while flying at other flight conditions. Being able to automatically and dynamically optimize a wing for any flight condition will result in less drag and reduced vehicle weight. With lower drag and weight, the vehicle's maximum range, speed and altitude will be increased.

For applications, high aspect ratio wings are used where low drag is desired. Because of their reduction in induced drag that is achieved with larger span. As the aspect ratio increases, the aero elastic phenomena become more important. Since adaptive flaps will typically be used in conjunction with high aspect ratio to reduce induced drag, it is important that the system of equation include static aero elastic effects, especially due to elastic twist. This study begins with relevant equations from Thin Aerofoil theory and Slender Beam theory. The equations from these theories were combined to get the closed form of solution that accounts for wing twist in the calculation of flap angles to create a desired c_l distribution along the wing. The method to find the structural properties through FEA is also presented. The structural properties are also calculated using standard Aircraft Structures method and the results were compared.

This study based on static aeroelastic effects, dynamic effects have been neglected due to following reasons:

- a) Inertial effects of wing have been neglected due to the low subsonic Mach number is active during the cruise.
- b) Wing twist due to self weight is very small hence rotational inertial effects can be neglected.
- c) Bending effect is ignored since it doesn't contribute to change in section angle of attack.
- d) For structural simplification the wing is modeled as a continuous shell with no flaps.

II. METHODOLOGY/MATHEMATICAL MODELING

2.1. Engineering data

The high aspect ratio wing has taken for analysis to demonstrate elastic twist properly. The example wing used in this chapter has an aspect ratio of 18, a wing area of 18 m^2 a taper ratio of 1, and operating at a Reynold's no 8.1×10^6 . There were 7 flaps placed on the trailing edge. In which 6 flaps of length 1.35m and the tip flap of length 0.9 m. The wing has zero geometric twist. The weight of the wing is assumed to be concentrated along the elastic axis, so it does not create a pitching moment.

Table.1: Parameters of wing

Parameter	Value
Aircraft Weight (W)	29376 N
Wing Area (S)	18 m ²
Wing Aspect Ratio (AR)	18
Taper Ratio	1
Wing Span (b)	18 m

Table.2: Material properties of aluminum alloy

Parameter	Value
Young's modulus (E)	7.24×10 ¹⁰ N/m ²
Shear modulus (G)	2.6×10 ¹⁰ N/m ²
Poisson's Ratio	0.33

A simple structural cross section of the wing was easily modeled in Catia software package, for the wing skin 3 mm, spar cap width 100 mm and spar thickness is 3 mm. The material properties of Aluminum alloy is given in table 2

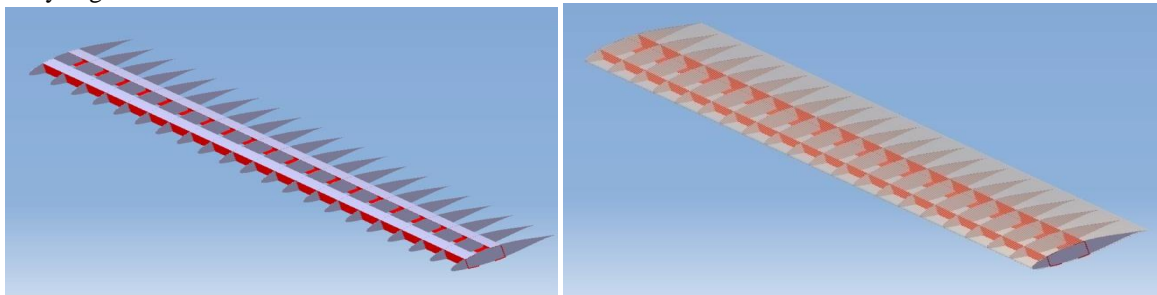


Fig.1: Wing structure without skin and with skin

2.2. Slender beam theory

In our analysis of an elastic wing, we have considered only the elastic twist of the wing. The wing itself is assumed to be unswept and of medium to very high aspect ratio, so that there are no chord wise deformations and twist and bending deformations were not coupled. Wing bending deformation has also been ignored in the development of the closed-form equations for determining the optimum flap angles, since bending does not contribute significantly to changes in the wing section angle of attack. This allows for the elasticity of the wing to be modeled as a simple torque tube.

The structure of the wing used consists of two interior webs and four spar caps at the junction of the skin and webs. This creates a three-cell thin-walled shell. Normally the flap is disconnected from the wing box, and does not add any structural rigidity to the wing. However, in order to simplify the finite element analysis (FEA) modeling, the outline of the airfoil is modeled. For structural purposes, wing has continuous shell with no flap.

According to Bispplinghoff the relationship between twist and torque for a beam is given by Equation 1

$$\{\theta\} = [C^{\theta\theta}] \{T\} \quad (1)$$

Both $\{\theta\}$ and $\{T\}$ are vectors with n elements. $C^{\theta\theta}$ is a square $n \times n$ influence coefficient matrix calculated using the below Equation 2. Each element of this matrix represents the twist caused at span wise station y due to a unit torque applied at another span wise location η

$$C^{\theta\theta}(y, \eta) = \int_0^y \frac{d\lambda}{GJ} \quad (\eta \geq y) \quad (2)$$

$$C^{\theta\theta}(y, \eta) = \int_0^\eta \frac{d\lambda}{GJ} \quad (y \geq \eta)$$

In the current work, two approaches were used to determine $C^{\theta\theta}$ using standard methods from aircraft structures to determine the torsional rigidity (GJ) of multi-cell structures.

Before calculating $C^{\theta\theta}$, the torsional stiffness(GJ) of the wing at every spanwise location needs to be calculated. The torsional constant, J for a three-cell thin-wall structure was calculated from the system of equations shown

in Equation 3. To solve for the torsional constant, the equations are arranged into matrix form as shown in Equation 5. The relationship between $G\theta$, τ , and J is shown in Equation 4.

$$\left. \begin{aligned} & [A_1 F_1] + [A_{21} F_2] + [A_2 F_3] = T \\ & \frac{1}{A_1} [-a_{10} F_1 + a_{12} (F_2 - F_1)] + 2G\theta = 0 \\ & \frac{1}{A_2} [-a_{20} F_2 + a_{21} (F_1 - F_2) + a_{23} (F_3 - F_2)] + 2G\theta = 0 \\ & \frac{1}{A_3} [-a_{30} F_3 + a_{32} (F_2 - F_3)] + 2G\theta = 0 \end{aligned} \right\} (3)$$

$$J = \frac{T}{G\theta} \quad (4)$$

$$\begin{bmatrix} A_1 & A_2 & A_3 & 0 \\ -a_{10} - a_{12} & a_{12} & 0 & 2A_1 \\ a_{21} & -a_{20} - a_{21} - a_{23} & a_{23} & 2A_2 \\ 0 & a_{32} & -a_{30} - a_{32} & 2A_3 \end{bmatrix} \begin{bmatrix} \frac{F_1}{\tau} \\ \frac{F_2}{\tau} \\ \frac{F_3}{\tau} \\ \frac{1}{J} \end{bmatrix} = \begin{bmatrix} \frac{1}{2} \\ 0 \\ 0 \\ 0 \end{bmatrix} \quad (5)$$

The area of each cell, A_i , and line integrals, a_{ij} are calculated from points located along the surface of the airfoil. F_i is the shear stress in the material surrounding A_i . The line integral (Equation 6) is calculated as the summation of several segments, with each segment being defined by two points. The distance between these two points is calculated and then divided by the thickness of the material for that segment. The line integral of each segment is then summed to give the total line integral between two areas.

$$a_{ij} = \int \frac{ds}{\tau} \quad (6)$$

The area of a cell is calculated by subdividing the cell into several triangles. The area for each triangle is calculated using standard methods.

2.3. Thin Airfoil Theory to Estimate Flap Effects

To minimize the profile drag of a wing, each wing section needs to be operating within the low-drag range (LDR) of lift coefficients (drag bucket) of the airfoil. The drag bucket occurs when the stagnation point is at or near the leading edge of the airfoil. Since a stagnation point has zero vorticity, we can describe the LDR mathematically through thin airfoil theory. We begin by defining $C_{l_{ideal}}$ as the C_l when the vorticity at the leading edge of an airfoil is zero. From airfoil theory, the vorticity along the camberline of an airfoil is given by Equation 8. The Fourier coefficients A_n were determined from Equation 9 and 10, and θ is the angular coordinate that corresponds to the chord wise coordinate, x , as defined by Equation 11. The lift coefficient was calculated from the vorticity through Equation 12. For the vorticity at the leading edge to be zero, A_0 was zero, which leads Equation 13 to calculate $C_{l_{ideal}}$. Because thin airfoil theory linearizes the aerodynamics, we determined the incremental effect of a trailing-edge flap deflection on $C_{l_{ideal}}$ using Equation 14, where θ_f is the angular location, in radians, of the flap hinge location.

$$\gamma(\theta) = 2V_\infty \left(A_0 \frac{1 + \cos(\theta)}{\sin(\theta)} + \sum_{n=1}^{\infty} A_n \sin(n\theta) \right) \quad (7)$$

$$A_0 = \alpha - \frac{1}{\pi} \int_0^\pi \frac{dz}{dx} d\theta_0 \quad (8)$$

$$A_n = \frac{2}{\pi} \int_0^\pi \frac{dz}{dx} \cos(n\theta_0) d\theta_0 \quad (9)$$

$$\theta = \cos^{-1} \left(1 - 2 \frac{x}{c} \right) \quad (10)$$

$$C_l = \pi (2A_0 + A_1) \quad (11)$$

$$C_{l_{ideal}} = 2 \int_0^{\pi} \frac{dz}{dx} \cos(\theta_0) d\theta_0 \quad (12)$$

$$\Delta C_{l_{ideal}} = 2\delta_f \sin(\theta_f) \quad (13)$$

III. RESULTS AND DISCUSSIONS

3.1. Calculation of lift and drag coefficients

The slope of the lift curve and the minimum drag range of the airfoil must be found to justify that we are operating in optimum drag range throughout our analysis. Since the aerodynamic analysis of the wing is done with Ansys-Fluent software, the same was used to find the c_l Vs α and c_l Vs c_d curve for two dimensional airfoil to standardize the analysis. From the analysis the airfoil was found operating in low drag range of 0.02 to 0.03 and the c_l Vs α relationship was linear in the range of -12° to 12° . For the CFD analysis the pressure far-field boundary condition was given and assumed standard conditions for aerofoil wall.

Fig. 2: Angle of Attack Vs Coefficient of lift for NACA 65-415

3.2. Lift Distribution over the semi-wing span

Methodology used in FLUENT

To calculate the lift distribution in Ansys Fluent package, the wing is divided into 10 small strips of



size 0.094m. The c_l value for the strip is calculated using Ansys Fluent. The c_p values were calculated at 12 sections. The c_l values obtained using the strips and using the wing sections was interpolated and the values are plotted against the wing span to obtain the lift distribution.

3.3. Rectangular wing with no flaps

The general lift distribution on the rectangular wing was calculated theoretically using the Fourier sine series method and computationally using FLUENT software. The Fourier co-efficients used are $A_1 \sin \theta$ & $A_3 \sin 3\theta$.

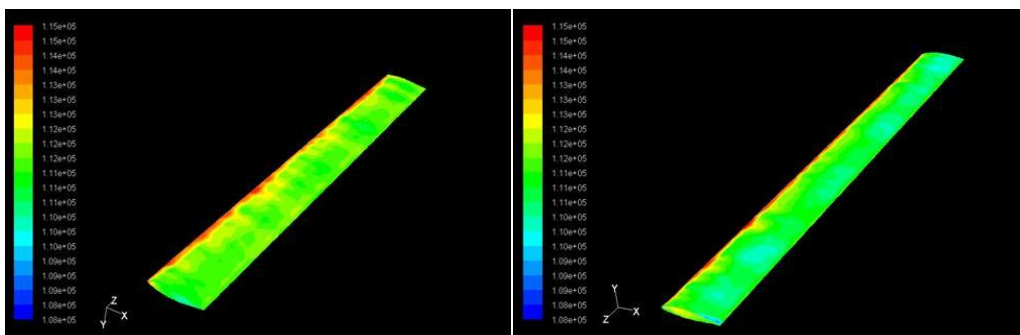


Fig.3: Pressure distribution in Pascal over lower and upper surface

The values obtained using theoretical methods and the computational methods are compared and given in figure 4.

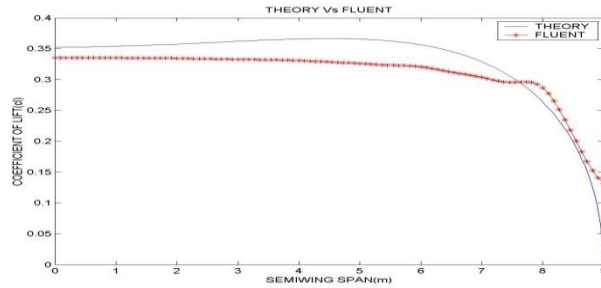


Fig. 4: Comparison of lift distribution theoretical Vs computational

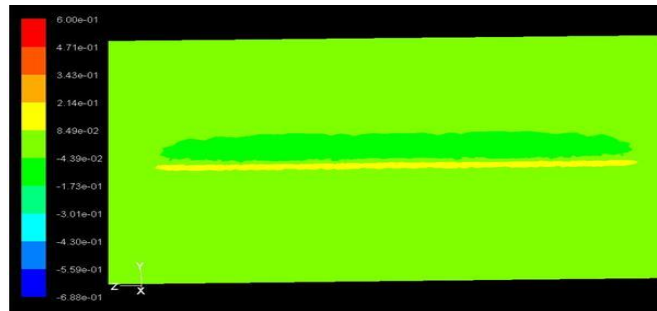


Fig. 5: Pressure variation over a wing span in Pascal

Regardingly the lift distribution occurs, the above pressure contours shows that the variation is almost constant all along the wing span except small variation at the tip.

3.4. Twisted wing with no flaps

The twisted wing geometry was generated using the multi-section surface method in Gambit software package. The twisted wing sections were rotated about their shear centre according to the twist value obtained using the FEA analysis.

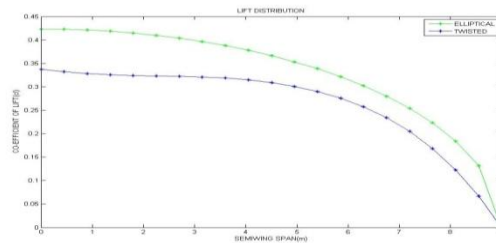


Fig. 6: Comparison of lift distribution theoretical Vs computational

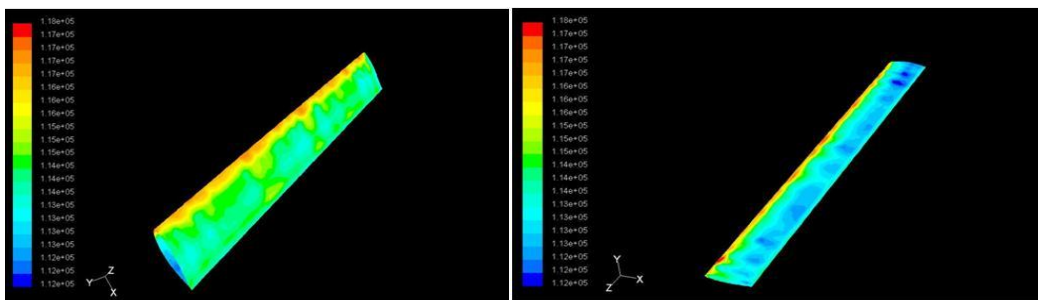


Fig. 7: Pressure distribution in Pascal over lower and upper side of twisted wing

3.5. Rectangular wing with multiple trailing edge flaps

The flap deflection angles were theoretically calculated using thin airfoil theory for every span wise location. Then mean flap angles were calculated and modeled in Gambit software package. The lift distribution for wing with flaps is computationally calculated in Fluent software package.

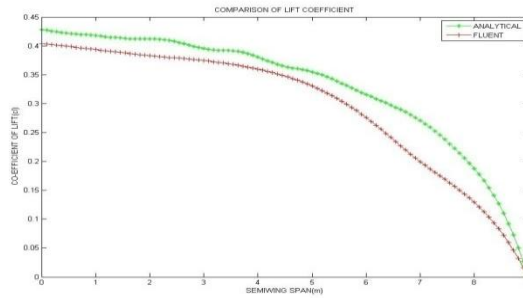


Fig. 8: Comparison of lift distribution theoretical Vs computational

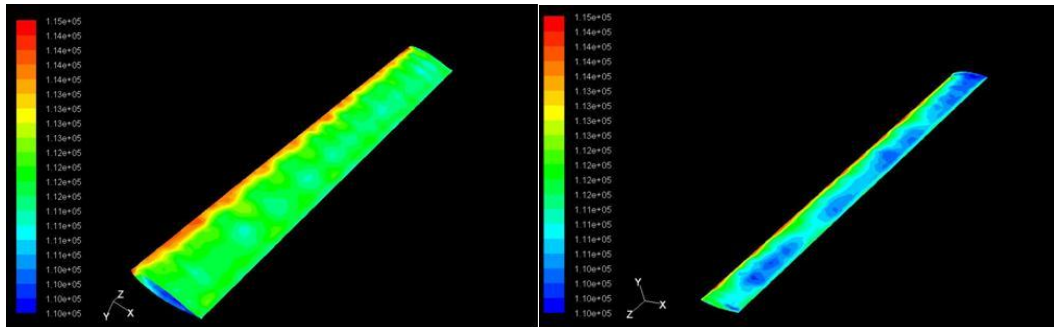


Fig. 9: Pressure distribution in Pascal over lower and upper side of twisted wing

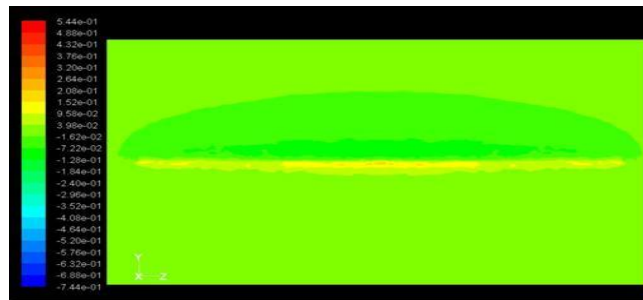


Fig. 10: Pressure variation over a wing span in Pascal

Regardingly the lift distribution occurs, the above pressure contours show that the variation is almost elliptical along the wing.

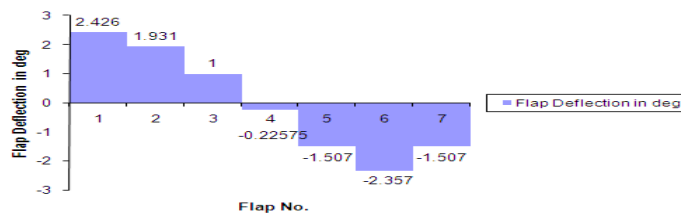


Fig. 11: Flap angles for rigid wing

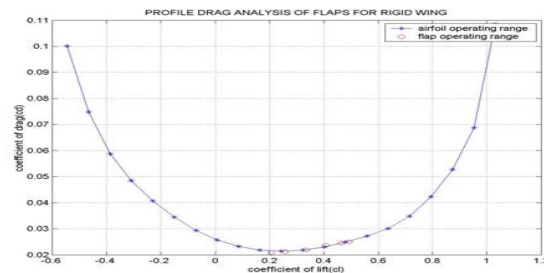


Fig. 12: Profile drag analysis for rigid wing

From above plot, all the flaps were operating at lower drag range.

3.6. Twisted wing with multiple trailing edge flaps

The flap angles required for the twisted wing were calculated using thin airfoil theory for every span wise location. The wing sections were rotated about their shear centre and the flaps were deflected at 80% of the total chord. The twisted wing sections were used to model the wing in Gambit software package by multi section surfaces. The lift distribution for the twisted wing with flaps deflected is calculated in Fluent software package. The values obtained using theoretical methods and the computational methods were compared in figure13

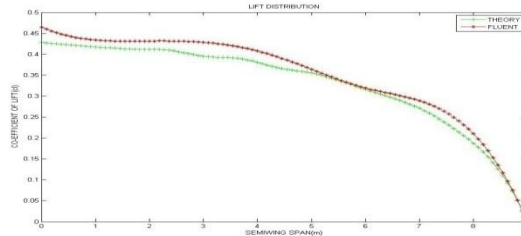


Fig. 13: Comparison of lift distribution theoretical Vs computational

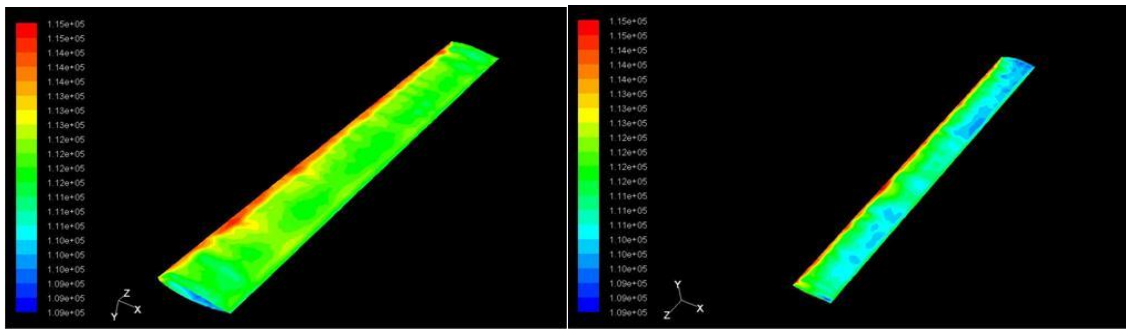


Fig. 14: Pressure distribution in Pascal over lower and upper side of twisted wing

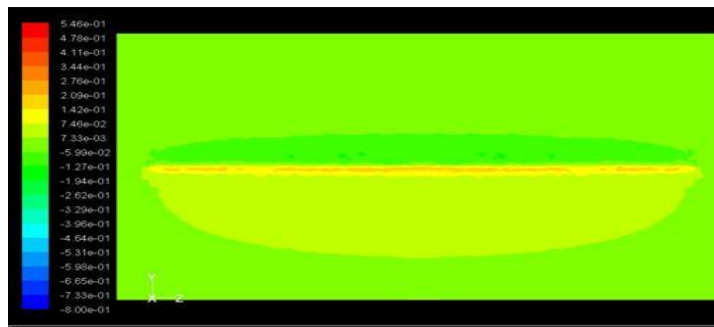


Fig. 15: Pressure variation over a wing span in Pascal

The above plot figure 15 shows the variation of coefficient pressure, in which the variation is almost elliptical along the twisted wing.

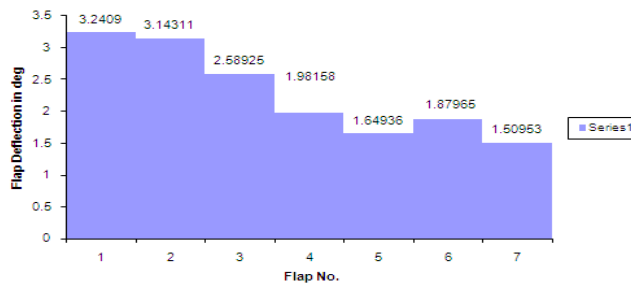


Fig. 16: Flap angles for twisted wing

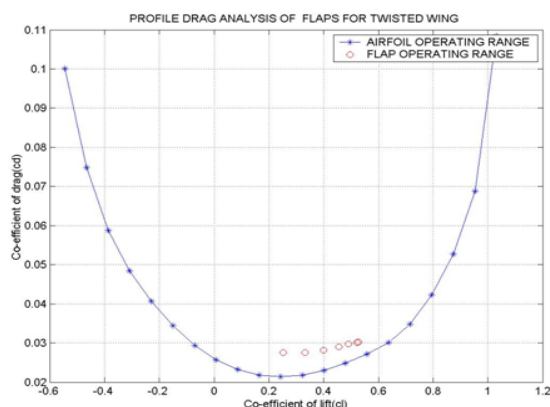


Fig. 17: Profile drag analysis for twisted wing

From above plot, all the flaps were operating at lower drag range.

3.7. Fluid structure interaction (FSI)

The FSI was used to study the interaction between flexible structure and the surrounding fluid for the stability analysis of airplane wings. Studying these phenomena requires modelling of both fluid and structure. Many approaches in computational Aeroelasticity seek to synthesize independent computational approaches for the aerodynamic and the structural dynamic subsystems. This strategy is known to be fraught with complications associated with the interaction between the two simulation modules. The task is to choosing the appropriate models for fluid and structure based on the application, and to develop an efficient interface to couple the two models. In the present article, FSI analysis was done by ANSYS software package. The wing was modelled in software package and aerodynamic analysis was done through ANSYS CFX package. The results were brought to structural simulation as loading conditions.

Boundary conditions were

Inlet- subsonic

Outlet- subsonic

Wing- no slip wall

Root end- symmetry

Air ideal gas

Viscous effect- k-epsilon method

Other sides – free slip wall

Reference pressure – 101325 Pascal

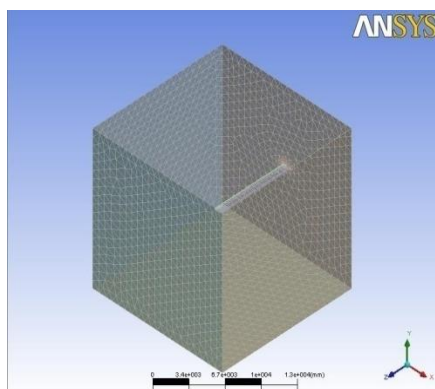


Fig. 18: FSI model with domain

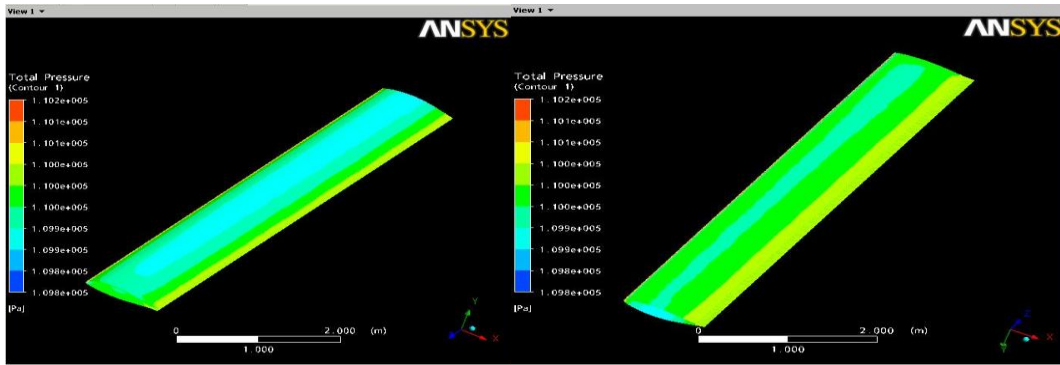


Fig. 19: Total pressure contours over upper and lower surface

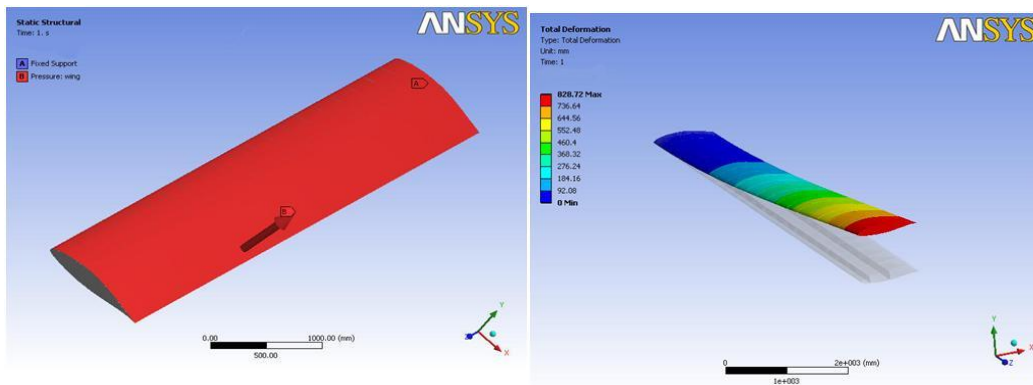


Fig. 20: FSI boundary conditions and total deformations

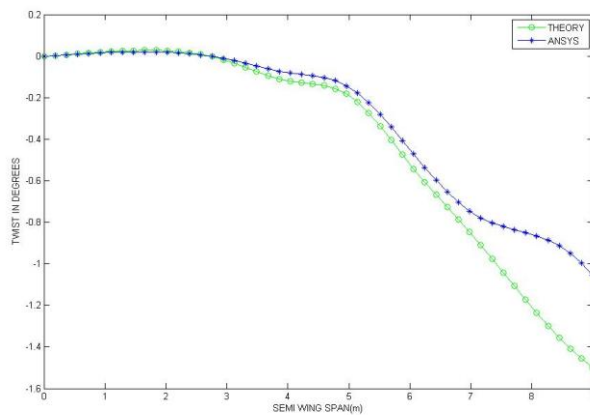


Fig. 21: Comparison of lift distribution theoretical Vs computational (ANSYS)

IV. CONCLUSION

The need for multiple trailing edge flaps was studied and the result derived from the analysis demonstrates the efficiency of multiple trailing edge flaps. Rigid and twisted wings were modeled with and without multiple trailing edge flaps. All those conditions were analyzed and results were compared both theoretically and computationally. Also profile drag analysis for the flaps have done through fluent software package and checked drag operating ranges. The design of aircraft with this concept clearly shows a breakthrough in the design with minimal changes in the existing technology. With advances in manufacturing technology, the concept will be an asset to aircraft industries. The scope of this study can be extended by adding more multiple trailing edge flaps in future. The non- linear aerodynamics and post stall behavior of the aircraft wing can be studied. Thus it makes the analysis more complicated. A more accurate picture can be obtained by undertaking a dynamic aero elastic analysis in future.

REFERENCES

- [1]. Thornton, S. V., "Reduction of Structural Loads using Maneuver Load Control in the Advanced Fighter Technology Integration (AFTI)/F-111 Mission Adaptive Wing", NASA TM 4526, September 1993.
- [2]. Bolonkin, A. and Gilyard, G. B., "Estimated Benefits of Variable-Geometry Wing Camber Control for Transport Aircraft", NASA TM 1999-206586, October 1999.
- [3]. Reich, G. W., Bowman, J. C., and Sanders, B., "Large-Area Aerodynamic Control for High-Altitude Long-Endurance Sensor Platforms," Journal of Aircraft ,2005.
- [4]. Spillman, J. J., "The use of variable camber to reduce drag, weight and costs Of transport aircraft," Aeronautical Journal, January 1992, pp 1-9
- [5]. Stanewsky, E., "Aerodynamic Benefits of adaptive wing technology," Aerospace Science and Technology, Vol. 4, 2000, pp. 439-452.
- [6]. Monner, H. P., Breitbach, E., Bein, T., and Hanselka, H., "Design aspects of the adaptive wing - the elastic trailing edge and the local spoiler bump," The Aeronautical Journal, February 2000, pp. 89-95.
- [7]. King, R. M. and Gopalathnam, A., "Ideal Lift Distributions and Flap Angles for Adaptive Wings," AIAA Paper 2004-4722, 22nd AIAA Applied Aerodynamics Conference, Providence, RI, August 2004.
- [8]. Jepsen, J. K. and Gopalathnam, A., "Computational Study of Automated Adaptation of a Wing with Multiple Trailing-Edge Flaps," AIAA Paper 20051035, 43rd AIAA Aerospace Sciences Meeting, Reno, NV, January 2005.
- [9]. Jones, R. T., "The Spanwise Distribution of Lift For Minimum Induced Drag Of Wings Having a Given Lift and a Given Bending Moment," NACA TN 2249, December 1950.
- [10]. Powers, S. G. and Webb, L. D., "Flight Wing Surface Pressure and Boundary Layer Data Report from the F-111 Smooth Variable-Camber Supercritical Mission Adaptive Wing," NASA TM 4789, 1997.
- [11]. Clarke, R., Allen, M. J., Dibley, R. P., Gera, J., and Hodgkinson, J., "Flight Test of the F/A-18 Active Aeroelastic Wing Airplane," NASA TM 213664, August 2005.
- [12]. Anderson Jr., J. D., Fundamentals of Aerodynamics, McGraw Hill, 3rd ed.,2001.
- [13]. Gene Hou, Jin Wang and Anita Layton., "Numerical Methods for Fluid-Structure Interaction" Communication of Computational Physics. Vol. 12, No. 2, pp. 337-377, August 2012
- [14]. R. van Loon, P.D. Anderson, F.N. van de Vosse, S.J. Sherwin, "Comparison of various fluid-structure interaction methods for deformable bodies", Department of Aeronautics, Imperial College London, South Kensington Campus, SW7 2AZ, London, UK
- [15]. RamjiKamakoti, Wei Shyy, "Fluid-structure interaction for aeroelastic applications", Progress in Aerospace Sciences 40 (2004) pp-535-558
- [16]. Edward N. Shipley, Jr. "static Aeroelasticity Considerations in Aerodynamic Adaptation of Wings for Low Drag", North Carolina State University
- [17]. Introduction to Aeroelasticity by Raymond L. Bisplinghoff and Holt Ashley and Robert L. Hoffmann
- [18]. Aerodynamics for engineers by Houghton and Carpenter, Butterworth-Heinemann, imprint of Elsevier science.
- [19]. Aircraft structure by Megson, Butterworth-Heinemann, Mar-2007. imprint of Elsevier science
- [20]. "The initial Torsional stiffness of shells with interior webs" by Kuhn. P (NACA TN 542)
- [21]. CATIA reference tutorial
- [22]. ANSYS FLUENT reference tutorial
- [23]. ANSYS CFX reference tutorial